Decay of three-dimensional acoustic turbulence and the resulting power spectrum for cosmological gravitational waves

Jani Dahl

June 19, 2024

Primordial first order phase transitions

- Primordial gravitational waves could have been sourced by first order phase transitions, such as one associated with the generation of the masses of elementary particles.
- Such transitions proceed by nucleation, expansion and merger of phase bubbles. The phase transition comes to an end when all the bubbles have merged with neighboring ones, leaving behind a characteristic spectrum of sound waves, which are an important source of primordial GWs.
- Even if not already present by the end of the transition, shocks develop with time from the steepening sound waves. A statistically random field of shock waves is called acoustic turbulence.

Fluid equations

The starting point is the relativistic equations of motion

$$\nabla_\nu T^{\mu\nu} = 0 \tag{1}$$

$$T^{\mu\nu} = T^{\mu\nu}_{\mathsf{PF}} + T^{\mu\nu}_{\mathsf{NPF}} \tag{2}$$

$$T^{\mu\nu}_{\mathsf{PF}} = (\rho + p)u^\mu u^\nu + pg^{\mu\nu} \tag{3}$$

$$T^{\mu\nu}_{\mathsf{NPF}} = -2\tilde{\eta}\sigma^{\mu\nu} \tag{4}$$

Expanding these to second order while assuming all quantities with units of velocity to be small in comparison to the speed of light with the ultrarelativistic equation of state

$$p = c_s^2 \rho \tag{5}$$

and constant kinematic shear viscosity gives...

Continuity equation

$$\frac{\partial \ln \rho}{\partial t} + (1 + c_s^2)\nabla \cdot \mathbf{v} + (1 - c_s^2)\mathbf{v} \cdot \nabla \ln \rho = 0 \tag{6}$$

Euler equation

$$\begin{aligned}\frac{\partial \mathbf{v}}{\partial t} + (\mathbf{v} \cdot \nabla)\mathbf{v} - c_s^2\mathbf{v}(\nabla \cdot \mathbf{v}) - c_s^2\mathbf{v}(\mathbf{v} \cdot \nabla \ln \rho) + \frac{c_s^2}{1 + c_s^2}\nabla \ln \rho \\ = \frac{\eta}{1 + c_s^2}\left[\nabla^2\mathbf{v} + \frac{1}{3}\nabla(\nabla \cdot \mathbf{v}) + 2\mathbf{S} \cdot \nabla \ln \rho\right]\end{aligned} \tag{7}$$

where

$$S_{ij} = \frac{1}{2}\left(\frac{\partial v_i}{\partial x_j} + \frac{\partial v_j}{\partial x_i} - \frac{2}{3}\delta_{ij}\nabla \cdot \mathbf{v}\right) \tag{8}$$

Numerical simulations and initial conditions

- Self-made 3D parallel MPI Python simulation code.
- The phase transition that precedes acoustic turbulence is not simulated in order to save computation time, and to ensure that the observed effects are not special to phase transitions.
- Initial conditions given in terms of longitudinal and transverse spectral densities. $P_\perp(k) = 0$ so that the flow is dominated by shocks.
- Velocity Fourier components are given random phases that correspond to random initial conditions.
- The initial energy density is uniform.

Universal shape for the energy spectrum

- Solving fluid equations for a single 1D shock $\rightarrow$ $\tanh$-profile.
- The energy spectrum can be written as

$$E(\kappa, t) = L(t)\mathcal{E}(t)\Psi(\kappa), \quad \kappa = L(t)k \tag{9}$$

  where $\mathcal{E} = \left\langle \mathbf{v}^2 \right\rangle / 2$ is the kinetic energy.

- Using the $\tanh$-profile, the spectral shape function can be written as

$$\Psi(\kappa) = \widetilde{\Psi}_0 \frac{(\kappa/\kappa_p)^{\beta+4}}{1 + (\kappa/\kappa_p)^{\alpha}} \mathcal{I}\left(\frac{\pi\kappa}{2\kappa_s}\right) \tag{10}$$

  where

$$\mathcal{I}(P) = \frac{1}{P}\frac{\cosh(P)}{\sinh^3(P)} \sim \begin{cases} \dfrac{1}{P^4}\,, & P \ll 1 \\ \dfrac{4}{P}e^{-2P}\,, & P \gg 1 \end{cases} \tag{11}$$

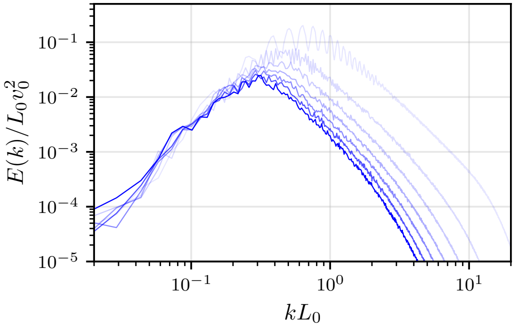

The scaled energy spectrum from simulation data plotted at various times. Dark colors correspond to late times.

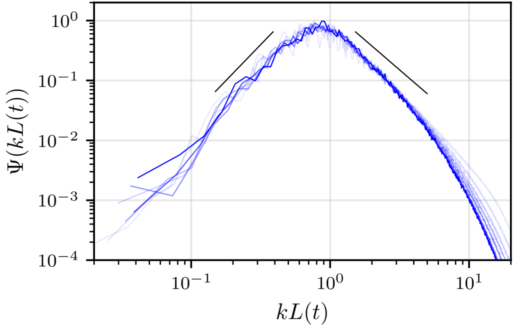

The same spectra collapsing into the function $\Psi(kL)$.

Kinetic energy decay

- Decay more complicated for acoustic turbulence than vortical. At late times, the mean decay rate set by the viscous dissipation.

- Solving the differential equation for the kinetic energy using the viscous dissipation term with the spectrum from previous slide and assuming a k^{-2} inertial range power law and stationarity of the spectrum at small wavenumbers gives

$$\mathcal{E}(t) = \frac{\mathcal{E}_0}{\left(1 + C\frac{t}{t_s}\right)^{\zeta}}, \quad \zeta = \frac{2(\beta+1)}{\beta+3} \tag{12}$$

and for the integral length scale it follows

$$L(t) = L_0 \left(1 + C\frac{t}{t_s}\right)^{\lambda}, \quad \lambda = \frac{2}{\beta+3} \tag{13}$$

Power law	All runs	Selected runs
$E(k)$: Inertial range	-2.44 ± 0.02	-2.31 ± 0.02
$E(k)$: Low wavenumber	3.44 ± 0.21	3.96 ± 0.12
Kinetic energy	-1.30 ± 0.01	-1.33 ± 0.01

Table 1: The averaged power law values for the inertial range power law $k^{\beta-\alpha}$ and the low wavenumber power law k^{β} of the energy spectrum, and the kinetic energy decay power law $t^{-\zeta}$ obtained from the 1000^3 resolution numerical simulations. In the selected runs column, only runs with Re > 40 have been taken into account for the inertial range, runs with Re < 60 for the low-k power law, and Run II has been excluded in the case of the kinetic energy decay power law for more optimal measurements. The expected values are -2, 4, and -10/7.

GW power spectrum

- We have approximated the GW power spectrum for acoustic turbulence by using the Gaussian approximation for the fluid velocity correlations and assuming departures from Gaussianity to be small.
- We also assume that the transition completes in much less than a Hubble time, meaning that the expansion of the universe can be neglected.
- The GW spectrum has been integrated numerically using the universal shape of the energy spectrum and the model for the decay.

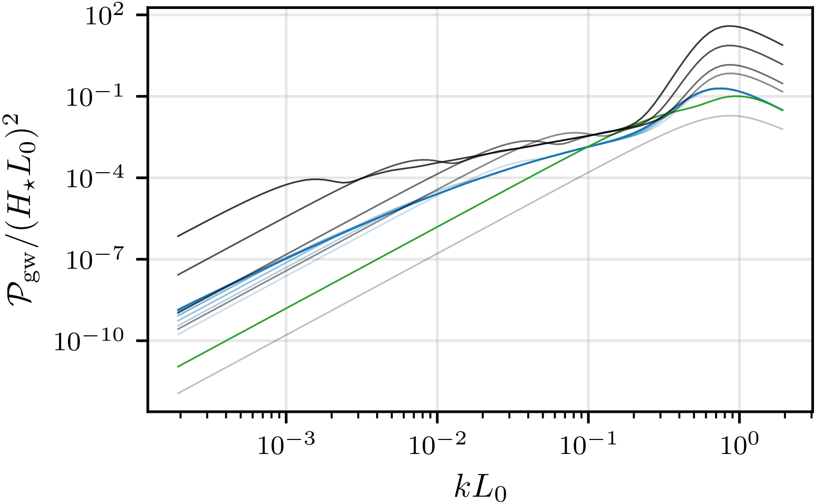

Figure 1: The converged spectra of the decaying case, colored in blue, plotted together with the stationary spectra ($C = 0$), colored in black, at times $t_{H_\star}/t_s \in [0.5, 2, 10, 20, 100, 520]$. The stationary spectrum at $t_{H_\star}/t_s = 2$ (green curve) coincides with the converged spectra of the decaying case at large wavenumbers. The chosen values for the free parameters are $\beta = 4$, $\bar{v}_0 = 0.2$, and $C = 0.2$.

$t_{H_\star}/t_s$	$L(t_{H_\star})/L_0$	p
21	1.60	4.66 ± 0.08
52	2.00	4.54 ± 0.05
104	2.41	4.24 ± 0.05
260	3.10	4.03 ± 0.03
520	3.78	3.99 ± 0.03
1039	4.60	3.98 ± 0.03
1559	5.16	3.98 ± 0.02
2078	5.60	3.98 ± 0.03

Table 2: The measured power law index p in the power law range k^p below the peak for the GW power spectrum $\mathcal{P}_{\rm gw}$ for different GW source durations. The fitting range is $kL_0 \in [0.28, 0.45]$. The measurements indicate a convergence in the power law towards k^4 at times for which $L(t_{H_\star})/L_0 \gtrsim 3.0$.

Summary

- The found decay properties ($\rightarrow t^{-10/7}$) and the universal shape of the fluid energy spectrum (broken power law with k^4, k^{-2}) are used to approximate the GW power spectrum of decaying acoustic turbulence.

- The decay is found to bring about a convergence in the spectral amplitude and the peak power law that leads to a shallower power law than the k^9 of the stationary case.

- For $\bar{v}_0 = 0.2$, $C = 0.2$ the power law has converged to k^4 at times for which $L(t_{H_\star})/L_0 > 3.0$.

- More careful study of the parameter space in terms of $\bar{v}_0$ and C and their potential effects on the power law value and convergence time, along with generalizing the calculation for the expanding universe case, is left as future work.

Backup slides

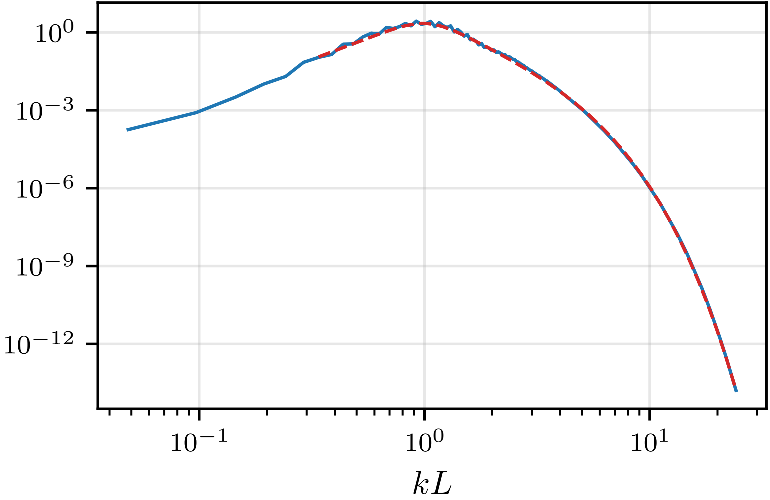

Figure 2: Fit (dashed red line) on the function $\Psi(\kappa)$ obtained from the longitudinal energy spectrum data of a $\mathrm{Re}_0 = 10$ run at $t = 20t_s$ using the previous equation as a fitting function. The obtained fit parameters are $\widetilde{\Psi}_0 = 0.61$, $\beta = 3.31$, $\alpha = 7.72$, $\kappa_p = 1.03$, and $\kappa_s = 2.65$.

ID	β_0	$\beta_0 - \alpha_0$	$\langle\beta\rangle_t$	σ_β	$\langle\alpha\rangle_t$	σ_α	$\langle\beta - \alpha\rangle_t$	$\sigma_{\beta-\alpha}$
I	5	−7	4.053	0.032	7.173	0.194	−3.120	0.213
II	4	−2	3.074	0.411	5.240	0.303	−2.165	0.124
III	4	−8	3.400	0.326	6.321	0.221	−2.920	0.125
IV	5	−4	3.959	0.181	6.442	0.185	−2.483	0.018
V	6	−14	4.270	0.187	6.875	0.192	−2.605	0.024
VI	6	−4	4.356	0.172	6.819	0.175	−2.463	0.013
VII	7	−19	4.384	0.432	6.766	0.428	−2.382	0.017
VIII	10	−5	4.178	0.541	6.572	0.509	−2.394	0.061
IX	3	−8	2.668	1.345	4.998	1.251	−2.330	0.102
X	5	−15	3.715	0.724	6.048	0.695	−2.333	0.043
XI	4	−12	3.184	0.908	5.521	0.865	−2.338	0.051
XII	2	−19	1.575	0.792	3.924	0.772	−2.349	0.034
XIII	3	−29	3.638	1.493	5.858	1.463	−2.220	0.050
XIV	2	−31	1.934	1.387	4.160	1.361	−2.227	0.034
XV	4	−48	3.231	1.120	5.439	1.105	−2.208	0.037

Table 3: Measured power laws and their time fluctuations from the simulations.

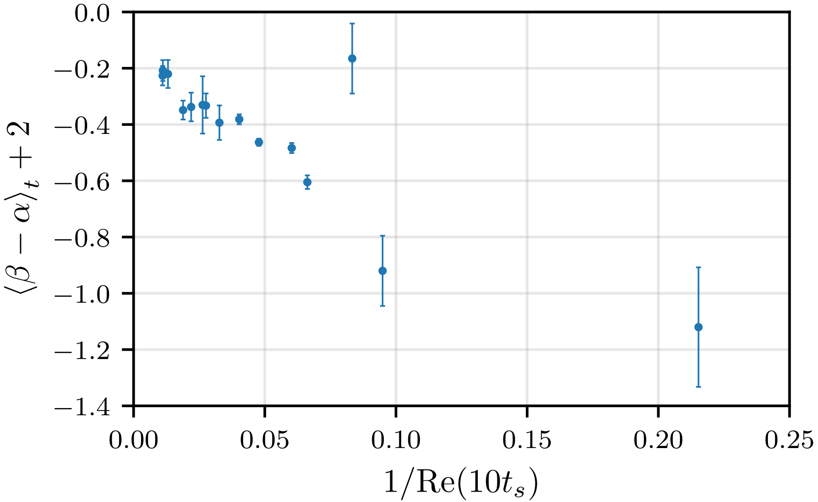

Figure 3: The scaled inertial range power law values $\langle\beta-\alpha\rangle_t$ of the previous table plotted against the Reynolds number at the middle of the averaging interval at $t=10t_s$. The standard deviations resulting from the time fluctuations are shown as error bars for each case.

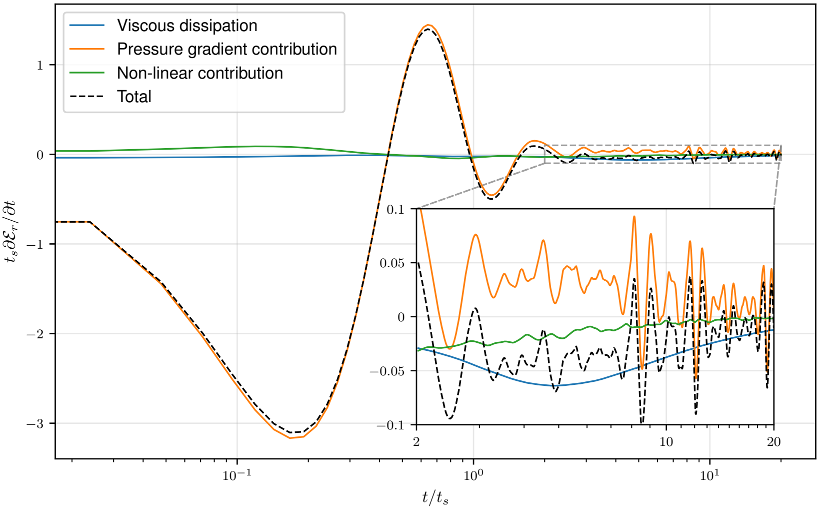

Figure 4: The dissipation rate of the kinetic energy fraction $\mathcal{E}_r(t) = \mathcal{E}(t)/\mathcal{E}_0$ resulting from the viscous dissipation, the pressure gradient, and the non-linear contributions measured in a simulation run.

ID	$\langle \zeta \rangle_t$	σ_ζ	ζ	$\langle C \rangle_t$	σ_C
I	1.497	0.019	1.433±0.003	0.240	0.006
II	0.891	0.016	1.341±0.045	0.517	0.023
III	1.257	0.014	1.375±0.032	0.243	0.005
IV	1.172	0.022	1.425±0.015	0.257	0.010
V	1.447	0.019	1.450±0.014	0.177	0.004
VI	1.313	0.022	1.456±0.013	0.206	0.006
VII	1.438	0.028	1.458±0.032	0.176	0.006
VIII	1.258	0.028	1.443±0.042	0.204	0.009
IX	1.059	0.031	1.294±0.167	0.289	0.019
X	1.318	0.034	1.404±0.064	0.193	0.010
XI	1.283	0.029	1.353±0.095	0.201	0.009
XII	1.317	0.043	1.126±0.151	0.200	0.013
XIII	1.448	0.074	1.397±0.136	0.169	0.016
XIV	1.402	0.101	1.189±0.228	0.186	0.026
XV	1.359	0.100	1.358±0.115	0.198	0.028

Table 4: Time averaged fit parameters for the kinetic energy power laws, and the decay constant C for each of the simulation runs.

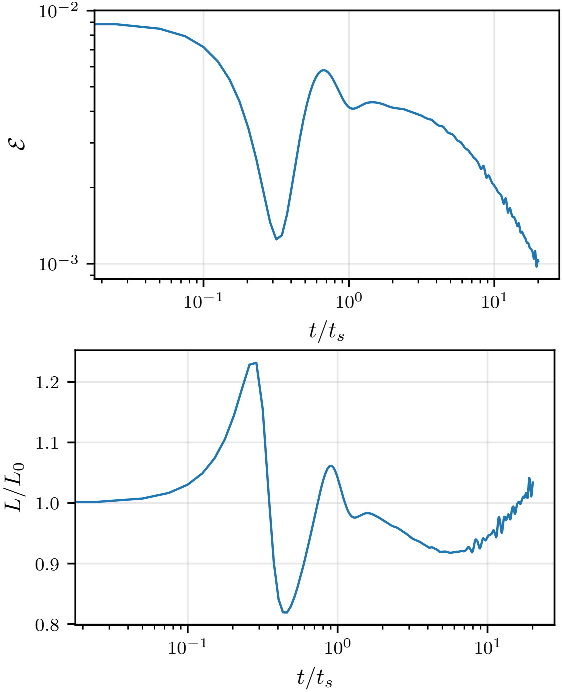
10^{-2}
10^{-3}
$\mathcal{E}$
10^{-1}
10^{0}
10^{1}
t/t_s
1.2
1.1
1.0
0.9
0.8
L/L_0
10^{-1}
10^{0}
10^{1}
t/t_s

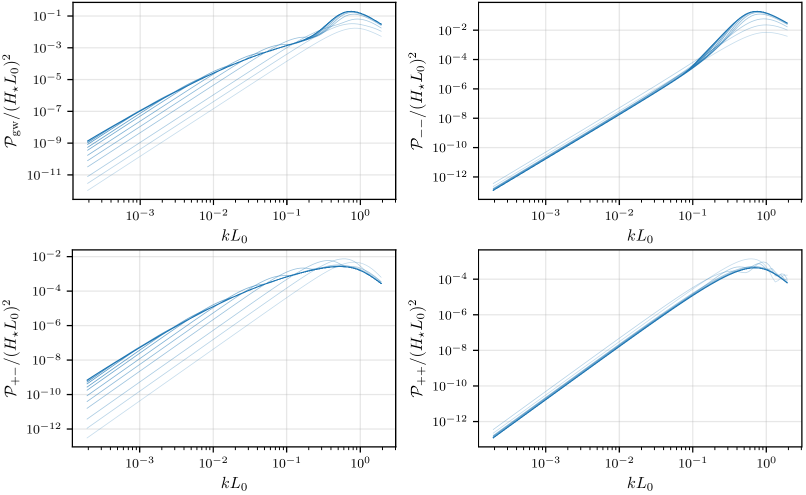

Figure 5: The total gravitational wave power spectrum and the components for various times obtained by numerical integration. The times in question are approximately $t_{H_\star}/t_s \in [0.5, 1, 2, 5, 10, 21, 52, 104, 260, 520, 1039, 1559, 2078]$, with dark lines corresponding to late times. The chosen values for the free parameters are $\beta = 4$, $\bar{v}_0 = 0.2$, and $C = 0.2$.